

# Molecular insight into $\gamma$ - $\gamma$ tubulin lateral interactions within the $\gamma$ -tubulin ring complex ( $\gamma$ -TuRC)

Charu Suri · Triscia W. Hendrickson ·  
Harish C. Joshi · Pradeep Kumar Naik

Received: 27 March 2014 / Accepted: 9 July 2014 / Published online: 17 July 2014  
© Springer International Publishing Switzerland 2014

**Abstract**  $\gamma$ -tubulin is essential for the nucleation and organization of mitotic microtubules in dividing cells. It is localized at the microtubule organizing centers and mitotic spindle fibres. The most well accepted hypothesis for the initiation of microtubule polymerization is that  $\alpha/\beta$ -tubulin dimers add onto a  $\gamma$ -tubulin ring complex ( $\gamma$ -TuRC), in which adjacent  $\gamma$ -tubulin subunits bind to the underlying non-tubulin components of the  $\gamma$ -TuRC. This template thus determines the resulting microtubule lattice. In this study we use molecular modelling and molecular dynamics simulations, combined with computational MM-PBSA/MM-GBSA methods, to determine the extent of the lateral atomic interaction between two adjacent  $\gamma$ -tubulins within the  $\gamma$ -TuRC. To do this we simulated a  $\gamma$ - $\gamma$  homodimer for 10 ns and calculated the ensemble average of binding free energies of  $-107.76$  kcal/mol by the MM-PBSA method

and of  $-87.12$  kcal/mol by the MM-GBSA method. These highly favourable binding free energy values imply robust lateral interactions between adjacent  $\gamma$ -tubulin subunits in addition to their end-interactions longitudinally with other proteins of  $\gamma$ -TuRC. Although the functional reconstitution of  $\gamma$ -TuRC subunits and their stepwise in vitro assembly from purified components is not yet feasible, we nevertheless wanted to recognize hotspot amino acids responsible for key  $\gamma$ - $\gamma$  interactions. Our free energy decomposition data from converting a compendium of amino acid residues identified an array of hotspot amino acids. A subset of such mutants can be expressed in vivo in living yeast. Because  $\gamma$ -TuRC is important for the growth of yeast, we could test whether this subset of the hotspot mutations support growth of yeast. Consistent with our model,  $\gamma$ -tubulin mutants that fall into our identified hotspot do not support yeast growth.

C. Suri · P. K. Naik (✉)  
Department of Biotechnology and Bioinformatics, Jaypee  
University of Information Technology,  
Waknaghat, Distt. Solan 173234, Himachal Pradesh, India  
e-mail: pknai1973@gmail.com

T. W. Hendrickson · H. C. Joshi  
Department of Cell Biology, Emory University School of  
Medicine, 447 Whitehead Biomedical Research Building,  
Atlanta, GA 30322, USA

*Present Address:*  
T. W. Hendrickson  
Department of Biology, Morehouse College, Atlanta, GA 30314,  
USA

*Present Address:*  
P. K. Naik  
Department of Biotechnology, Guru Ghasidas Vishwavidyalaya  
(A Central University), Koni, Bilaspur 495 009, Chhattisgarh,  
India

**Keywords** Gamma tubulin ·  $\gamma$ -TuRC · Protein–protein  
interaction · MD simulation · MM-PBSA · MM-GBSA

## Introduction

$\gamma$ -tubulin is a small globular protein and is most noticeably localized at the microtubule organization centers (MTOC) in eukaryotes [1–6].  $\gamma$ -tubulin was first discovered by Oakley and Oakley, in *Aspergillus* as the third member of the tubulin super-family [7]. Unlike  $\alpha$  and  $\beta$ -tubulins,  $\gamma$ -tubulin does not polymerize into the microtubule lattice, but is instead recruited to the microtubule organizing centers [5, 6]. Microtubules, composed primarily of  $\alpha/\beta$ -tubulin heterodimers, are key component of mitotic spindle apparatus necessary for the segregation of duplicated chromosomes into daughter cells during cell division. They

also play a vital role in many other cellular functions including the establishment of cell polarity, cell motility, intracellular organelle transport and maintenance of the overall cellular morphology. Such a myriad of roles calls for a very rapid reorganization. Microtubule assemblies, obtained *in vitro* from purified tubulin, differ from microtubule assemblies *in vivo* in both their structural lattice and the constrained initiation of assembly at the specific locations [8]. *In vitro*, disassembly is energetically favored over the assembly process until a critically large oligomer is formed [9]. Cells overcome this slow initial phase of the assembly process by providing specific nucleation sites called microtubule organization centers, which in most animal cells is a centrosome [10]. Experimental methods have shown that  $\gamma$ -tubulin interacts with the minus end of the microtubules [11].  $\gamma$ -tubulin is present at the MTOC's of eukaryotes as a large multisubunit complex called the  $\gamma$ -tubulin ring complex ( $\gamma$ TuRC) as a unit for microtubule assembly nucleation [13]. This complex is composed among other proteins of relatively smaller complexes called the  $\gamma$ -tubulin small complex ( $\gamma$ TuSC).  $\gamma$ TuSC is composed of two copies of  $\gamma$ -tubulin and one copy each of gamma complex protein 2 (GCP2) and gamma complex protein 3 (GCP3) [12]. Multiple copies of  $\gamma$ TuSCs along with GCP4, GCP5 and GCP6 associate together to form the larger  $\gamma$ TuRC [13]. Among the multiple proposed hypothetical models, the 'template model' is widely accepted that presents a ring of  $\gamma$ -tubulin on top of the  $\gamma$ TuRC as the template. In this model, each  $\gamma$ -tubulin subunit interacts laterally with another  $\gamma$ -tubulin unit and longitudinally with the  $\alpha/\beta$ -tubulin subunits to form the microtubules lattice. The mode of interaction of  $\gamma$ -tubulin with  $\alpha/\beta$ -tubulin as well as  $\gamma$ -tubulin is not complete. Therefore, in the present study we have made an attempt to explore the molecular basis of  $\gamma$ - $\gamma$  tubulin lateral interactions. Agard et al. (2008) deciphered the crystal form of  $\gamma$ -tubulin bound to GDP (PDB: 3CB2, Resolution 2.3 Å) that contained two subunits of  $\gamma$ -tubulin, pointing to the existence of a  $\gamma$ - $\gamma$  tubulin dimer *in vivo* [9]. Hence, the molecular interactions between the two  $\gamma$ -tubulin units in the dimer were studied utilizing *in silico* molecular modelling and molecular dynamics (MD) methods. Molecular dynamics is one of the predominant approaches to theoretically study bio-molecules. It allows the study of time dependent behaviour of molecular systems computationally and furnishes a wealth of thermodynamic and energetic information. Therefore, in recent years, MD simulation has gained lot of popularity in elucidating protein–protein interactions [14–19]. The robustness of protein–protein interactions have been quantified in terms of binding free energy. Binding free energies in solution can be calculated using the molecular mechanics Poisson–Boltzman solvation area (MM-PBSA) and molecular mechanics generalized Born solvation area

(MM-GBSA) approaches [20–23]. Generalized Born (GB) model has been successfully used to determine the energy contributions of each residue in the complex to identify the binding hotspot amino acids [14–16, 24]. To verify binding hotspots, virtual alanine scanning might be employed to obtain the difference in the free energy of binding between the alanine mutants and the wild types. Therefore in this endeavour we elucidated the protein–protein interactions between adjacent  $\gamma$ -tubulin using molecular dynamics simulations followed by MMPB/GB-SA and *in silico* alanine scanning mutation analyses. Findings were further validated using computational alanine scanning mutation analyses.

## Materials and methods

### Computational methods

#### *Molecular system*

The initial coordinates of  $\gamma$ -tubulin homodimer (PDB ID: 3CB2, Resolution 2.3 Å) [9] were obtained from Protein DataBank (PDB). The structure contained two chains of  $\gamma$ -tubulin ('A' and 'B') with 446 amino acids each. During the initial screening of the  $\gamma$ -tubulin dimer many errors such as many missing residues and missing side chains were observed. Therefore, it was imperative to fix these structural anomalies before proceeding with further molecular modelling calculations. Forty-three residues of chain A and 51 residues of chain B were found to be missing and represented gaps in the crystal structure. To reconstitute the homodimer only the 'A' chain was used from the crystal structure. In the 'A' chain, 14 residues were missing from three different locations (278–283, 311–312 and 367–371) while remaining 15 residues were missing from the terminals (1 from N terminal and 14 from C terminal). The three non-terminal gaps were filled following homology modelling using multiple templates in Prime (version 3.0, Schrödinger).

The modelled structure was subjected to energy minimization in Macromodel (version 9.9, Schrödinger) using Polak-Ribiere Conjugate Gradient (PRCG) algorithm and OPLS 2005 force field with a gradient of 0.001 kcal/mol and 1,000 steps of iterations. The resultant structure was then optimized using protein preparation wizard (PPrep, Schrödinger). Missing side chains were filled using Prime (version 3.0, Schrödinger). The structure obtained was energy minimized using OPLS 2005 force field with PRCG algorithm. The minimization was stopped either after 5,000 steps or after the energy gradient converged below 0.001 kcal/mol.

To further refine the structure, a small run of all atom Molecular Dynamics (MD) simulations was carried out for

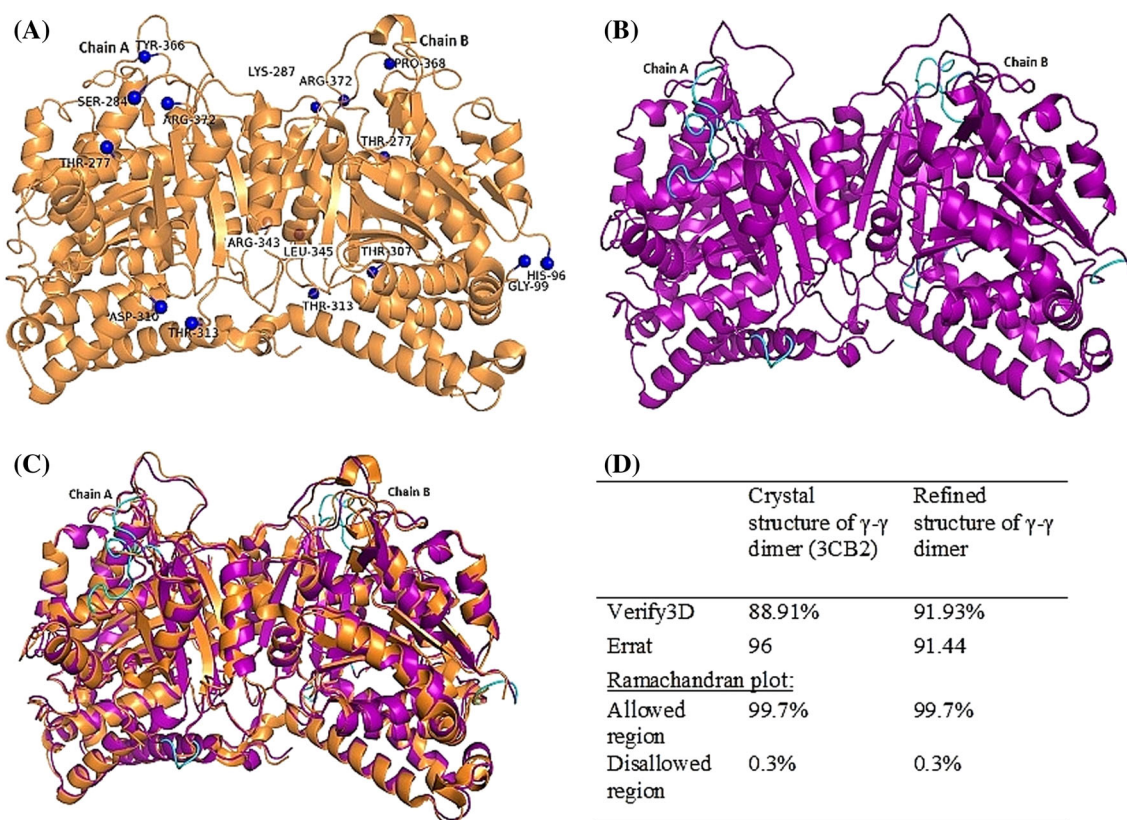


**Fig. 1** Crystal structure of  $\gamma$ - $\gamma$  dimer and its refined structure. Panel 'a' shows the crystal structure of  $\gamma$ - $\gamma$  dimer (PDB ID: 3CB2) with gaps. Gap flanking residues are shown as blue spheres. Panel 'b' shows the refined structure of  $\gamma$ - $\gamma$  dimer. A total of 14 missing residues were added and these can be seen in cyan colour. Panel 'c'

shows the refined structure of  $\gamma$ - $\gamma$  dimer (purple) superimposed over the initial crystal structure of  $\gamma$ - $\gamma$  dimer obtained from 3CB2 (orange); calculated RMSD was 0.73 Å. Panel 'd' gives the structure quality parameters of both the wild type and refined structure of  $\gamma$ - $\gamma$  dimer

1,000 ps with a time step of 2 fs on the modelled structure using Gromacs package (Version 4.5.4) [25]. The simulations were set up with AMBER ff99SB force field, in a dodecahedron solvation box at a distance of 12 Å from the periphery of the protein with simple point charges (spc216 model) of water molecules, using periodic boundary conditions [26]. Particle-Mesh-Ewald algorithm was employed to calculate the electrostatic interactions between atoms [27, 28]. The Lenard-Jones and electrostatic interaction cut-off were set at 1.0 nm distance. LINCS algorithm was used to constraint the bond lengths [29]. Prior to the 1,000 ps MD simulation the molecular system was neutralized with 9 Na<sup>+</sup> ions, energy relaxed using steepest descent algorithm for 1,000 steps and then equilibrated for 100 ps of MD run. An average structure was generated using the last 200 frames from the total of 1,000 frames generated during MD simulation. The  $\gamma$ - $\gamma$  dimer was then reconstituted by substituting the coordinates from the refined structure of 'A' chain onto the original crystal structure, preserving the original geometry and orientation (Fig. 1). Furthermore, the  $\gamma$ - $\gamma$  dimer obtained was energy minimized. The overall quality of the reconstituted  $\gamma$ - $\gamma$

homodimer was determined using PROCHECK [30, 31], ERRAT [32] and VERIFY3D [33].

#### Molecular dynamics simulations of the $\gamma$ - $\gamma$ complexes

In order to study the molecular interactions in  $\gamma$ - $\gamma$  complex, the dimer structure reconstituted above was simulated using Molecular Dynamics in Amber 11.0 and Ambertools 1.5 [34, 35]. The proteins were prepared for simulations using Leap program implemented in Ambertools. In leap, AMBER ff99SB [36, 37] force field was assigned to proteins, hydrogens were added, counter ions were added to neutralize the system and protein system was solvated using TIP3P water model in an octahedral box with a span of 15.0 Å from the periphery of the protein [38]. The molecular system was made to go through three consecutive rounds of energy minimizations to relax the molecular system and to remove any disallowed "bad" contacts. In each 1,000 step minimization, protein was first minimized for 500 steps using steepest descent method followed by 500 steps using conjugate gradient with a time step of 2 fs. In the first and second rounds positions restraints of 10 and

2 kcal<sup>-1</sup> Å<sup>-2</sup> respectively, were imposed on the protein system to allow relaxation of solvent molecules. Third minimization was carried out with no restraints. The system was gradually heated from 0 to 300 K. The system was then equilibrated for 500 ps at 300 K and 1 atm pressure. After all the thermodynamic properties were stabilized, the molecular system was simulated for 10 ns with a time step of 2 fs. For MD simulations, isobaric (NPT) conditions were maintained with the target pressure of 1 bar utilizing the Berendsen barostat [39]. The temperature was regulated using Langevin thermostat. All electrostatic interactions were described using Particle Mesh Ewald (PME) [27, 28] method and all bonds were constrained using Shake algorithm [29]. The non-bonded cutoff distance was kept at 10 Å. Co-ordinates were written to the trajectory file every 2 ps to obtain a total of 5,000 frames. All trajectories were analysed using PTRAJ program implemented in amber-tools [40].

#### Theoretical binding affinity calculation

The calculation of binding free energy in solvation, between the  $\gamma$ -tubulin units in the dimer was determined using the conventional MM-PBSA and MM-GBSA approaches described in Amber 11 [20, 41]. Out of the total 5,000 frames obtained during MD simulation 250 frames were extracted every 20 ps from last 5 ns of the MD trajectory for calculation of the ensemble average of binding free energy. The binding free energy was calculated considering each molecular species (complex, receptor and ligand) and the binding free energy was calculated as follows.

$$\Delta G_{\text{bind}} = \Delta G_{\text{complex}} - [\Delta G_{\text{protein}} + \Delta G_{\text{lig}}]$$

The free energy,  $G$ , for each molecular species was calculated by the following MM-PBSA and MMGBSA methods described in Amber.

Gibbs's free energy ( $G$ ) for each molecular species was calculated as follows:

$$G = E_{\text{gas}} + G_{\text{sol}} - TS$$

$T$  and  $S$  are the temperature and the total solute entropy, respectively.  $E_{\text{gas}}$  describes the gas phase energy and represents the sum of internal energy, van der Waals interaction energy and electrostatic interaction energy. It is calculated using parameters described in the Amber FF99SB force field [36, 37].

$$E_{\text{gas}} = E_{\text{int}} + E_{\text{ele}} + E_{\text{vdw}}$$

$G_{\text{sol}}$  describes the free energy of solvation and was calculated as the sum of polar and nonpolar solvation contributions as described below:

$$G_{\text{sol}} = G_{\text{PB(GB)}} + G_{\text{sol-np}}$$

$G_{\text{PB(GB)}}$  describes the polar solvation contribution and are obtained solving the Poisson–Boltzman (PB) and Generalized Born (GB) equations [20, 41].

Total polar interaction contributions were obtained as the sum of the electrostatic energy components and polar solvation components as given below:

$$G_{\text{ele,PB(GB)}} = E_{\text{ele}} + G_{\text{PB(GB)}}$$

The non-polar solvation contribution ( $G_{\text{sol-np}}$ ) was estimated using 0.0,072 kcal mol<sup>-1</sup> Å<sup>-2</sup> as the value for constant  $\gamma$  and by determining the solvent-accessible surface area (SAS) using a water probe radius of 1.4 Å [42]

$$G_{\text{sol-np}} = \gamma_{\text{SAS}}$$

Dielectric constants for solute and solvent were set to 1 and 80, respectively.

#### Energy decomposition and computational alanine scanning

Binding free-energy contributions of each residue at the protein–protein interaction interface were calculated using the GB model, implemented in Amber11, on the basis of 250 snapshots extracted every 20 ps from the last 5 ns of MD simulation trajectory [43, 44]. On the basis of individual contributions to the binding free energy of the complex, those amino acids contributed more significantly to the binding free energy (contribution >2.0 kcal/mol) were considered as the hotspot amino acids. These hotspot amino acids were believed to contribute most to the stability of complex and are significant for the  $\gamma$ - $\gamma$  tubulin interaction.

To further study the energy contribution of these amino acids in the interaction of  $\gamma$ - $\gamma$  tubulin, computational alanine scanning was performed. In this method an amino acid of interest is replaced with alanine and absolute binding free energy is recalculated. In our study the hotspot amino acids were mutated to alanine and binding free energies were calculated for the resulting mutated system using the MM-GBSA approach on the 250 snapshots extracted every 20 ps from the last 5 ns of MD simulation. Finally, the difference in the binding free energies of the mutant and wild type,  $\Delta\Delta G_{\text{bind}}$ , was computed as follows:

$$\Delta\Delta G_{\text{bind}} = \Delta G_{\text{bind}}[\text{Mutant}] - \Delta G_{\text{bind}}[\text{Wild Type}]$$

Positive values of  $\Delta\Delta G_{\text{bind}}$  indicate the favourable contribution while negative values indicate unfavourable contributions.

#### Preparation of mutant structure of $\gamma$ - $\gamma$ tubulin homodimer

To further investigate the molecular interactions between  $\gamma$ - $\gamma$  tubulin homodimer a stretch of polar amino acids (Arg339, Arg341, Glu342, Arg343 and Lys344) at the interface of  $\gamma$ - $\gamma$  dimer were mutated to alanine. Due to

their polar nature and their location at the interface of the  $\gamma$ - $\gamma$  dimer, this stretch of polar amino acids would play an important role in binding of two  $\gamma$  tubulin subunits. To precisely investigate the role of this stretch of amino acids in the binding of the  $\gamma$ -tubulin units, computational site directed mutagenesis was performed. All the five amino acids in the prepared structure of  $\gamma$ - $\gamma$  dimer were mutated to alanine using Maestro interface in Schrodinger. The mutant structure was then optimized and energy minimized for 5,000 steps with OPLS 2005 force field and PRCG algorithm using Macromodel (Schrödinger). Furthermore, a 10 ns MD simulation was performed on the resultant structure in Amber keeping the method and parameters consistent with those used for the wild type. After 10 ns simulation, the ensemble average of the theoretical binding affinity was calculated for the last 5 ns mutant complex trajectories using the MM-PBSA and MM-GBSA methods.

## Experimental methods

### Experimental alanine scanning mutation and phenotypes

pALTER-EX1 vector (Promega, Madison, WI) was used to subclone *TUBG1* cDNA into the *NdeI* site downstream from the SP6 promoter to create pTWH101 as described by Hendrickson et al. [45]. Based on our findings from the molecular modelling studies, a stretch of five polar amino acids (Arg339, Arg341, Glu342, Arg343 and Lys344) that contributed significantly to the lateral  $\gamma$ - $\gamma$  tubulin interactions were mutated to alanine by oligonucleotide-directed mutagenesis using pTWH101 as the template. pALTER-EX1 contains a tetracycline resistance gene and an inactivated ampicillin resistance gene. The ampicillin-repair oligonucleotide restores the activity of the inactivated AmpR gene, and the tetracycline knockout oligonucleotide inactivates the TetR gene. This schema, i.e., inactivation of the TetR gene and the activation of the AmpR gene, provided a rapid method for selecting potential alanine-scanning mutants. Because contiguous alanine codons can be used to create a *PstI* site, we used *PstI* digestion to further screen for potential alanine-scanning mutants. We then verified the mutated sequences that represented the only differences between the mutant (*tubg1*) and the wild type (*TUBG1*).

The yeast expression plasmids were constructed by subcloning each of the *tubg1* alleles into pREP1 at the *NdeI* site downstream of the *nmt1* + promoter [46, 47]. Wild type cells [48] were transformed with either one of the *tubg1*-pREP1 plasmids or the control *TUBG1*-pREP1 and grown in minimal media supplemented with adenine, histidine, and uracil. Transformants were screened at 18 and 36 °C to identify conditional mutants in the presence of endogenous  $\gamma$ -tubulin. The strains were maintained at 30 and 26 °C, respectively. A diploid strain, NC377 [4, 49], bearing one endogenous wild-

type copy of *S. pombe*  $\gamma$ -tubulin, *gtb1* + and one disrupted copy, *gtb1::ura4* +, was also transformed with the mutant plasmids. The resulting yeast transformants were randomly sporulated and selected for *ura* +, *leu* +, and the spores were tested for conditional growth.

## Results and discussion

### Refinement of $\gamma$ - $\gamma$ tubulin dimer structure

The original crystal structure of  $\gamma$ - $\gamma$  tubulin dimer (PDB ID: 3CB2, resolution 2.3 Å) has missing amino acids (we called as gaps) at certain places (Fig. 1a). These gaps were filled based on the homology model building and the  $\gamma$ - $\gamma$  tubulin dimer was reconstituted and refined further by performing 10 ns MD simulation (Fig. 1b, c). The overall quality of the model obtained, stereo-chemical values and non-bonded interactions were tested using PROCHECK, ERRAT and VERIFY3D. The PROCHECK results showed 99.2 % of backbone angles are in allowed regions with G-factors of  $-0.25$ . Ramachandran plot analysis revealed only 0.3 % residues in the disallowed region (Fig. 1d). ERRAT is an “overall quality factor” calculator program for non-bonded atomic interactions. The accepted range in ERRAT is 50 and higher scores indicate the precision of the model. In the case of  $\gamma$ - $\gamma$  tubulin dimer, the ERRAT score was 91.43 % that is within the range of high quality model. Similarly, the VERIFY 3D score of 91.93 indicates a good quality model.

### Structural stabilities from MD simulations

To decipher the molecular insight of the interaction of  $\gamma$ - $\gamma$  tubulin dimer we have performed MD simulation of 10 ns. The relative fluctuation in the root-mean-square deviations (RMSDs) of the C $\alpha$  atoms of  $\gamma$ - $\gamma$  tubulin dimer is very small after the initial equilibration ( $\sim 4$  ns), demonstrating the stability of the molecular system (Fig. 2). To further test the convergence of the system we have monitor the root mean square fluctuation (RMSF) of the amino acids. As can be seen from Fig. 3, the fluctuations of individual amino acids are very small ( $<3.0$  Å) along the whole trajectory except 2 amino acids: Arg285 and Tyr365 (with RMSF  $>3.0$  Å) in chain ‘A’ and Val285, Arg311 and Gln312 (with RMSF  $>3.0$  Å) in chain ‘B’. The small fluctuation in RMSF reveals that the system is stable during the monitored molecular dynamics simulation.

### Analysis of calculated binding free energy

The molecular interaction and binding free energy between  $\gamma$ - $\gamma$  tubulin dimer was calculated based on MM-PBSA and

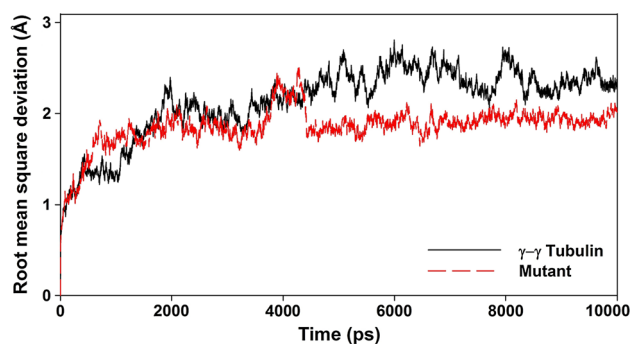


**Fig. 2** Root mean square deviation of  $\gamma$ - $\gamma$  tubulin complex and mutant complex with respect to time over 10,000 picoseconds

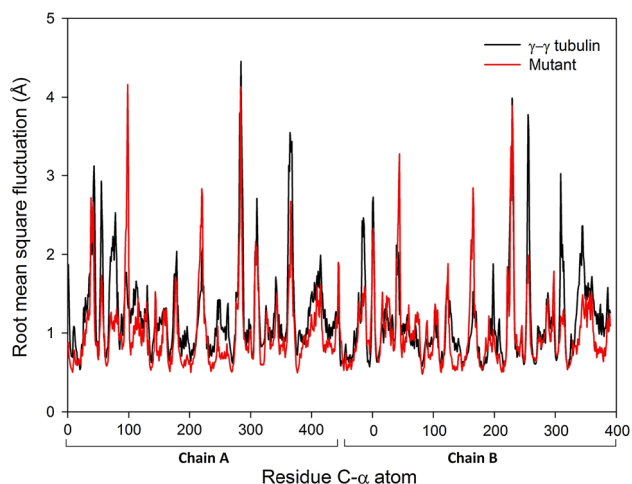


**Fig. 3** Root mean square fluctuations of residue C $\alpha$  atom over 10,000 picosecond

MM-GBSA of the MD trajectories. Both the methods indicated very robust interactions between the two  $\gamma$ -tubulin subunits (Table 1). The ensemble average of binding free energy using MM-PBSA and MM-GBSA was determined as  $-107.76$  and  $-87.12$  kcal/mol. The difference in the values obtained could be attributed to the calculated polar solvation energy which was  $749.15$  kcal/mol obtained by MM-GBSA, higher than  $726.91$  kcal/mol as obtained using MM-PBSA. Energy value was calculated as the average value of 250 snapshots, generated every 10 ps, from the last 5 ns of the MD trajectory. All molecular interactions in polar solvent are guided by polar (the polar interaction,  $\Delta G_{(ele,PB/GB)} = \Delta E_{ele} + \Delta G_{(PB/GB)}$ ) and non-polar energy components. The non-polar component generally yields a more favourable contribution as compared to the polar component to the molecular interactions as the non-polar residues have the tendency to bury themselves in the hydrophobic pockets allowing the water in the binding site to displace [50]. However, these non-polar forces are not strong enough to steer the association of two proteins.

**Table 1** Ensemble average of binding free energy (kcal/mol) of  $\gamma$ - $\gamma$  tubulin complex calculated using the MM-GBSA and MM-PBSA methods in Amber

Contribution	$\gamma$ - $\gamma$ complex	Mutant $\gamma$ - $\gamma$ complex
$\Delta E_{int}$	0.00	0.00
$\Delta E_{vdw}$	$-158.10$	$-155.06$
$\Delta E_{ele}$	$-676.57$	$410.33$
$\Delta E_{gas}$	$-834.67$	$255.27$
$\Delta G_{sol-np}$	$-18.70$	$-17.68$
$\Delta G_{PB}$	$745.61$	$-324.61$
$\Delta G_{solv, PB}$	$726.91$	$-342.28$
$\Delta G_{ele, PB}$	$69.04$	$85.72$
$H_{tot, PB}$	$-107.76$	$-87.02$
$\Delta G_{GB}$	$770.11$	$-316.08$
$\Delta G_{solv, GB}$	$749.15$	$-335.44$
$\Delta G_{ele, GB}$	$93.55$	$94.25$
$H_{tot, GB}$	$-85.52$	$-80.17$

Therefore charge residues are often found to be located at the protein–protein interaction interface as they play a key role in electrostatic steering which can be explained as a long range electrostatic mechanism that might lead to recognition of the binding interface [51]. As evident from Table 1, though the Coulombic contributions  $\Delta E_{ele}$  of  $-676.57$  kcal/mol are highly favourable to binding, they cannot compensate the large penalty imposed by the desolvation component ( $\Delta G_{PB/GB}$ ) of  $745.61$  and  $770.11$  kcal/mol as calculated by MM-PBSA and MM-GBSA, respectively. The non-polar components comprising of van der Waals interaction contribution ( $\Delta E_{vdw}$ ) and the non-polar solvation contribution ( $\Delta G_{sol-np}$ ) were estimated to be highly favourable with the values of  $-158.10$  and  $-18.70$  kcal/mol respectively. This highly favourable non-polar component might explain the solute–water dispersion and the hydrophobic effects.

Decomposition of the binding free energy into the per residue contribution

To further understand the  $\gamma$ - $\gamma$  interactions at the atomic level, binding free energy contributions were determined for each residue in the  $\gamma$ - $\gamma$  complex using the MM-GBSA method and plotted in Fig. 4. The residues having a contribution of  $>2$  kcal/mol were considered as hotspot amino acids and they were positioned to contribute most to the stability of the  $\gamma$ - $\gamma$  complex. As an example Asp252, Met249, His334 of chain ‘A’ and Arg341, Met249, Asp252 of chain ‘B’ make very high free energy contributions  $>4$  kcal/mol hence, making considerably large contribution to the overall binding free energy of the complex. In addition to these residues, seven more residues of chain ‘A’ (Arg341, Arg265, Trp446, Ile 444, Tyr443, Pro353, Asn250) and nine amino acids of

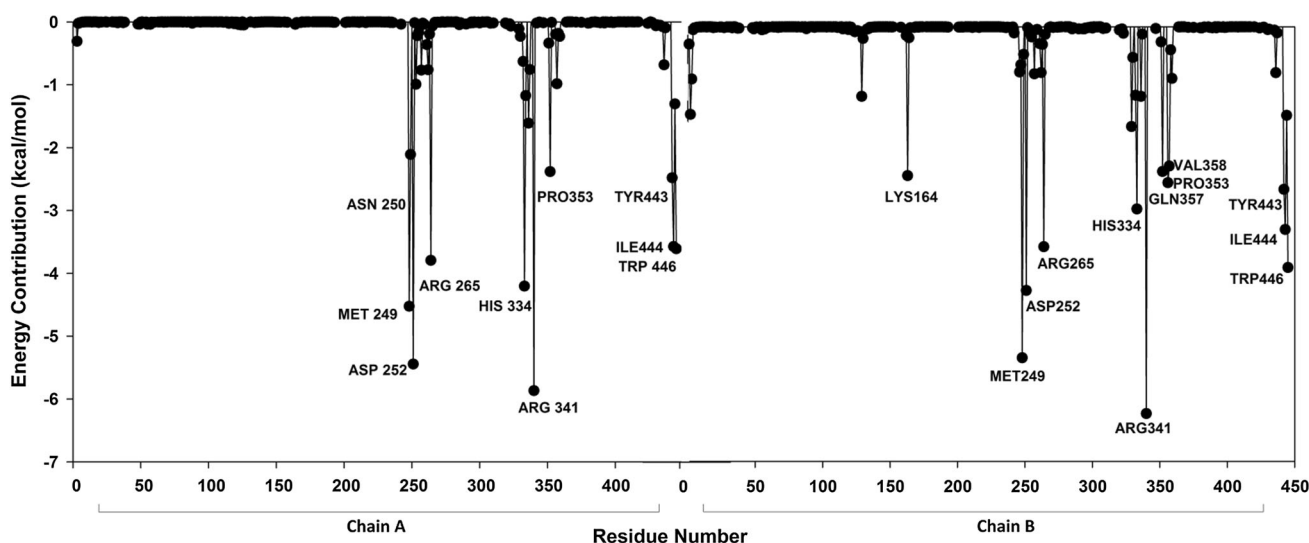


**Fig. 4** Per residue energy contribution of amino acids to the stability of  $\gamma$ -tubulin dimer, calculated using the MM-GBSA method

chain ‘B’ (Arg265, His334, Tyr443, Gln357, Lys164, Pro353, Val358, Ile444, Trp446) show high energy contribution  $>2$  kcal/mol.

Significantly, all the hotspot amino acids were observed to lie at the  $\gamma$ - $\gamma$  complex interface (Fig. 5). Furthermore, to determine the detailed contribution of each important residue, the binding energy was decomposed into several other components like the electrostatic, van der Waals, solvation and total contribution (Table 2). Most hotspot amino acids like Met249, Asn250, Arg265, Trp446 of chain ‘A’ and Met249, His334, Trp446 of chain ‘B’ were observed to make significant non-polar contributions ( $>4$  kcal/mol). However, some residues like Asp252, Arg265 of chain ‘A’ and residues Lys164, Asp252, Arg265 and Arg341 of chain ‘B’ were observed to make considerable polar contributions ( $>2$  kcal/mol) (Fig. 6). Arginine is a versatile amino acid which is capable of forming different types of favourable interactions like hydrogen bond and salt bridge formation. Arg341 and Arg 265 of chain ‘A’ forms two hydrogen bonds with Asp252 and Trp446 of chain ‘B’, respectively, while Arg341 and Arg265 of chain ‘B’ forms four hydrogen bonds each with Asp252 and Trp446 of chain ‘A’ (Fig. 7). The occurrence of H-bond throughout the 10 ns simulation is described in Table 3.

#### Computational alanine scanning

To further determine the contribution of hotspot amino acids identified above to binding free energy between  $\gamma$ - $\gamma$  interactions we performed computational alanine scanning. The method proposes that a minute local change in the protein does not affect the overall conformation of the protein–protein complex. The results obtained by the decomposition of

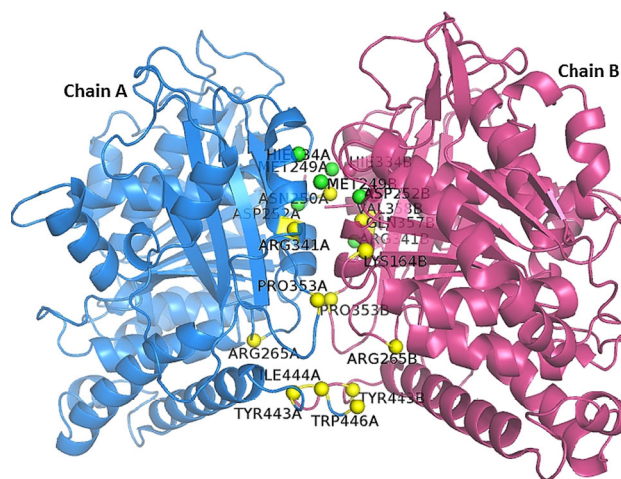


**Fig. 5** Hot spot amino acids. Energy contribution of each amino acid to the stability of the  $\gamma$ - $\gamma$  tubulin dimer calculated using the MM-GBSA method. C- $\alpha$  atoms of amino acid residues contributing  $>4$  kcal/mol are marked green spheres while those with a contribution of 2–4 kcal/mol are marked yellow

the binding free energy and computational alanine scanning were found to be quite consistent and this indicates the reliability of our analysis. After performing computational alanine scanning for hotspots and, a substantial decrease in the binding free energy was observed. The mutation to alanine led to a decrease in the binding affinity, for each hotspots amino acid, at least by 1.16 kcal/mol, while for Asp252 of chain ‘A’ as well as Asp252 and Arg341 of chain ‘B’, the binding free energy was decreased by more than 10 kcal/mol using both MM-PBSA and MM-GBSA methods, thereby reducing the strength of  $\gamma$ - $\gamma$  tubulin lateral association (Table 4). This reiterates that the hotspots amino acids identified in the interaction between  $\gamma$ - $\gamma$  subunits are very crucial.

**Table 2** Decomposition of calculated  $\Delta G_{\text{bind}}$  (kcal/mol) on per residue basis into van der Waals, electrostatic, polar solvation and non-polar solvation energy components

	Residue	$\Delta E_{i,\text{vdw}}$	$\Delta E_{i,\text{ele}}$	$\Delta G_{i,\text{sol GB}}$	$\Delta G_{i,\text{sol-np}}$	$\Delta H_{i,\text{tot,GB}}$
Chain A	MET249	-6.93	-4.61	8.20	-1.19	-4.53
	ASN250	-4.80	-12.12	15.63	-0.83	-2.11
	ASP252	-0.50	-40.48	35.85	-0.31	-5.45
	ARG265	-0.34	-66.03	62.85	-0.27	-3.80
	HIE334	-4.92	1.26	0.21	-0.75	-4.20
	ARG341	-2.91	-101.4	101.2	-0.80	-5.87
	PRO353	-2.39	-2.60	3.12	-0.50	-2.38
	TYR443	-3.44	-2.16	3.48	-0.36	-2.48
	ILE 444	-3.11	-2.51	2.51	-0.47	-3.58
	TRP 446	-6.72	49.44	-45.05	-1.28	-3.61
	Chain B	LYS164	-0.07	5.71	-7.90	-0.14
MET249		-6.45	-3.78	6.07	-1.18	-5.33
ASP252		-0.66	-24.97	21.49	-0.11	-4.25
ARG265		-0.51	-67.09	64.34	-0.28	-3.54
HIE334		-4.39	-3.34	5.51	-0.72	-2.93
ARG341		-1.24	-102.5	98.15	-0.63	-6.23
PRO353		-2.33	-2.75	3.23	-0.49	-2.33
GLN357		-1.63	-6.28	5.65	-0.25	-2.51
VAL358		-2.08	-2.73	2.78	-0.22	-2.24
TYR443		-3.61	-2.14	3.53	-0.40	-2.62
ILE 444		-2.89	-2.34	2.42	-0.45	-3.27
TRP446		-6.94	49.51	-45.12	-1.34	-3.88

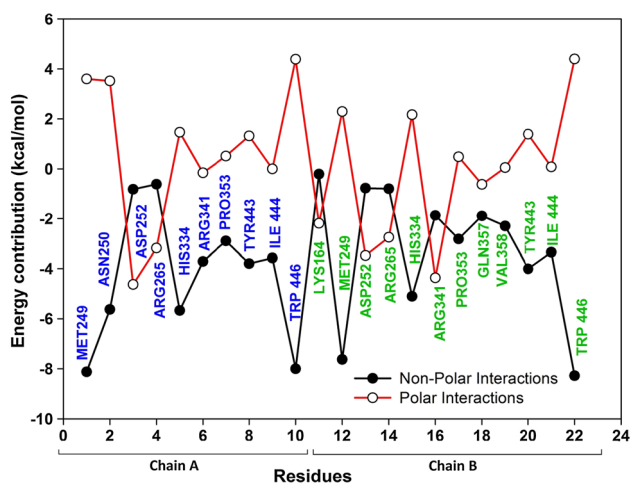


**Fig. 6** The polar and the non polar contributions of residues of chain A (labelled blue) and chain B (labelled green) in the  $\gamma$ - $\gamma$  tubulin dimer calculated using MM-GBSA method

Predicted binding free energy between mutant  $\gamma$ - $\gamma$  subunits

To develop a refined model of lateral  $\gamma$ - $\gamma$  tubulin dimer interactions in the  $\gamma$ TuRC and in the absence of purified  $\gamma$ - $\gamma$  tubulin dimer, alternatively we have computationally modelled a mutant structure of  $\gamma$ - $\gamma$  homodimer by mutating a stretch of 5 polar amino acids (Arg339, Arg341,

Glu342, Arg343 and Lys344) to Alanine at the interface of  $\gamma$ - $\gamma$  dimer (Fig. 8) and recalculated the binding free energy between mutated  $\gamma$ - $\gamma$  dimer. Besides, Arg341 of chain 'B' has a tendency to form multiple H-bonds with Asp252 of chain 'A' at the binding interface. Hence calculated binding free energy of mutant  $\gamma$ - $\gamma$  subunits using both MM-PBSA and MM-GBSA methods led to substantial decrease in the total free energy of binding in comparison to wild type  $\gamma$ - $\gamma$  homodimer. The total binding free energy of the wild type predicted using MM-GBSA ( $H_{\text{tot, GB}}$ ) and MM-PBSA ( $H_{\text{tot, PB}}$ ) methods was decreased from  $-85.52$  and  $-107.76$  to  $-80.17$  and  $-87.02$  kcal/mol respectively for the mutant  $\gamma$ - $\gamma$  tubulin homodimer. The van der Waal's contribution was comparable for both wild type ( $-158.10$  kcal/mol) and mutant ( $-155.06$  kcal/mol) structures. In contrast, the electrostatic contribution of the mutant structure was found to be less favourable ( $410.33$  kcal/mol) compared to wild type ( $-676.57$  kcal/mol). This was anticipated as the polar amino acids which contributed to the total electrostatic contribution were changed to Alanine. There was noticeable rearrangement in the hydrogen bonding pattern between the mutant  $\gamma$ - $\gamma$  tubulin dimer. Overall the number of hydrogen bonds decreased compared to wild type as shown in Fig. 9.

The experimental production and a functional experimental test of a  $\gamma$ - $\gamma$  tubulin dimer is currently not feasible. Fortunately, because the function of  $\gamma$ -tubulin is essential

**Fig. 7** 2D representation of molecular interactions between the amino acids of the two units of  $\gamma$ - $\gamma$  tubulin (*chain 'A'* and *chain 'B'*). Hydrogen bonding residues are shown in green and red for *chain A* and *chain B*, respectively. The Dashed lines denote hydrogen bonds, and numbers indicate hydrogen bond lengths in Å. Hydrophobic interactions are shown as arcs with radial spokes. The Figs was made using Dimplot [52]

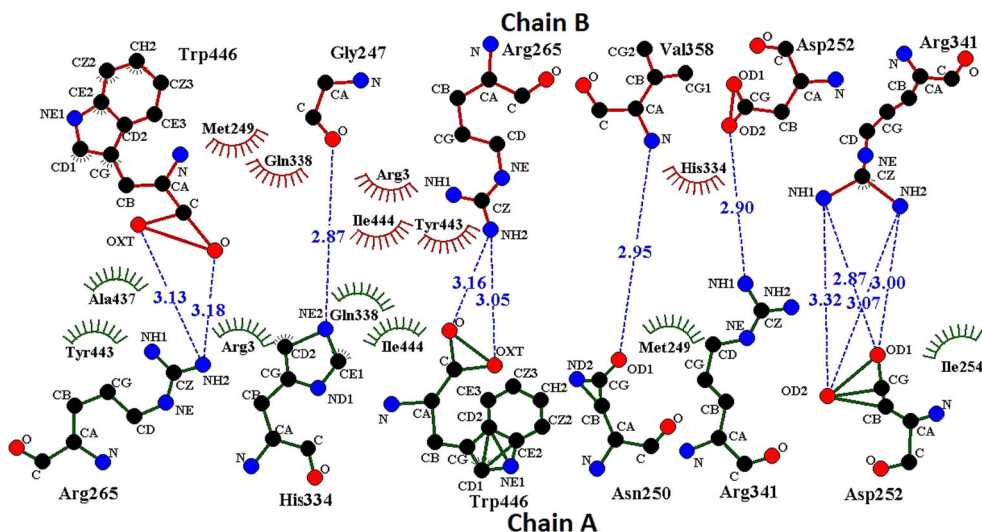


**Table 3** Occurrence (%) of H-bond between the two  $\gamma$ -tubulin units during the 10 ns MD simulation

Chain	Donor residue	Donor atom	Chain	Acceptor residue	Acceptor atom	Occurrence (%)	Distance (Å)
A	Asp252	OD1	B	Arg341	NH1	81.1	2.9
					NH2	69.4	2.9
					NH2	71.5	3
					NH1	58.1	3.1
	Trp446	OXT	Arg265	NH2	56.6	2.9	
B	Gly247	O	A	His444	NE2	85.6	2.9
					OD1	Arg3	NH1
	Asp252	OD2	Arg341	NH1	NH1	92.3	2.9
					NH2	30.5	3
					NH2	48	2.9
Trp446	OXT	Arg265	NH2	NH2	42	2.9	

for viability and growth of organisms that express it, this allows at least a test of viability in vivo. Therefore we sought to further test the effect of changing the entire cluster of Arg339, Arg341, Glu342, Arg343 and Lys344 to alanine and then test whether, when expressed in the living organism (unicellular fission yeast, *S. pombe*), it can support viability and growth (see below).

**Growth of Alanine scanning mutant in fission yeast and its phenotype**

$\gamma$ -tubulin, a highly evolutionarily conserved protein, is required for cell division and growth and its loss is lethal in yeast. However, some mutations that perturb  $\gamma$ -tubulin function produce conditional growth phenotypes [7, 48]. Since we were interested in identifying evolutionarily conserved features of  $\gamma$ -tubulin, we took advantage of the fact that the human  $\gamma$ -tubulin gene (*TUBG1*) can replace

the fission yeast  $\gamma$ -tubulin (*gtb1*). Using alanine-scanning mutagenesis, a series of  $\gamma$ -tubulin mutants, which targeted key residues predicted to be involved in protein–protein interactions, were generated. To test the effect of the selected alanine substitution on protein function haploid yeast cells, wild-type and *gtb1*-, were transformed with the alanine mutants. Wild-type *TUBG1* transformants served as controls. It was observed that the  $\gamma$ - $\gamma$  tubulin mutant (*gtb1*-alanine-*TUBG1*) was unable to support growth in the absence of endogenous *gtb1*+ (referred to as recessive lethal). This might be attributed to the mutation of key polar residues to alanine that intercepted the molecular recognition between adjacent  $\gamma$ -tubulins which led to malformation of the  $\gamma$ TuSC and hence the mitotic spindle.

Therefore, some key features predicted by our computational model are also consistent with mutant data that show the featured key amino acid residues (hotspot), when mutated and expressed into living yeast are insufficient to

support the growth and hence cell division of the yeast cell. These observations are consistent with our model although more comprehensive in vitro assembly data will be

**Table 4** Computational alanine scanning results for hotspot residues at the interface between  $\gamma$ - $\gamma$  tubulin dimer

	Hotspot residues	$\Delta\Delta G_{GB}$	$\Delta\Delta G_{PB}$	
Chain A	MET249	6.43	6.15	
	ASN250	4.67	5.67	
	ASP252	17.5	25.0	
	ARG265	6.72	7.22	
	HIE334	7.52	4.80	
	ARG341	10.1	11.8	
	PRO353	1.72	1.70	
	TYR443	3.32	1.26	
	ILE 444	3.11	1.39	
	TRP 446	2.9	1.42	
	Chain B	LYS164	1.16	1.20
		MET249	6.75	5.74
		ASP252	10.9	29.8
ARG265		6.52	7.07	
HIE334		3.01	1.16	
ARG341		13.4	16.6	
PRO353		1.70	1.78	
GLN357		2.86	3.15	
VAL358		1.28	2.15	
TYR443		3.70	2.29	
ILE 444		2.94	1.24	
TRP446		2.8	1.2	

The hotspot residues at the interface between  $\gamma$ - $\gamma$  tubulin dimer were mutated one at a time and recalculated the binding free energy of the mutant using both MM-GBSA and MM-PBSA methods

necessary for further experimental validation of the model of the  $\gamma$ - $\gamma$  tubulin interactions within the  $\gamma$ TuRC.

## Conclusions

In this study, the molecular basis of interaction between two lateral  $\gamma$ -tubulin units within the  $\gamma$ TuRC were elucidated by making extensive use of molecular mechanics and molecular dynamics techniques. A refined structure of  $\gamma$ - $\gamma$  tubulin homodimer was obtained based on the initial coordinates from the PDB (PDB\_ID: 3CB2, Resolution: 2.3 Å). The refined structure was MD simulated to obtain a 10 ns trajectory that was utilized to perform MM-PBSA/GBSA calculations and binding free-energy decomposition analyses in order to characterize interactions between two  $\gamma$ -tubulin units. MM-PBSA and MM-GBSA calculations revealed highly favourable non-polar component. Although some Columbic contribution were found to be favourable and probably played a crucial role in the binding site recognition, the overall polar contribution was less significant to the overall binding free energy due to penalty imposed by very large desolvation energy component. Therefore, the non-polar component was considered as the driver of the molecular interactions between  $\gamma$ - $\gamma$  tubulin. Also, on the basis of per residue free energy decomposition a total of twenty-two hotspot amino-acids were identified which were found to contribute highly (>2 kcal/mol) to the binding affinity between the two  $\gamma$ -tubulins. Computational alanine scanning was carried out for these hotspot amino acids resulted in a drop of at least 1.16 kcal/mol for each hotspot amino acid. On the basis of these findings, a mutant structure of  $\gamma$ - $\gamma$  tubulin homodimer was obtained after

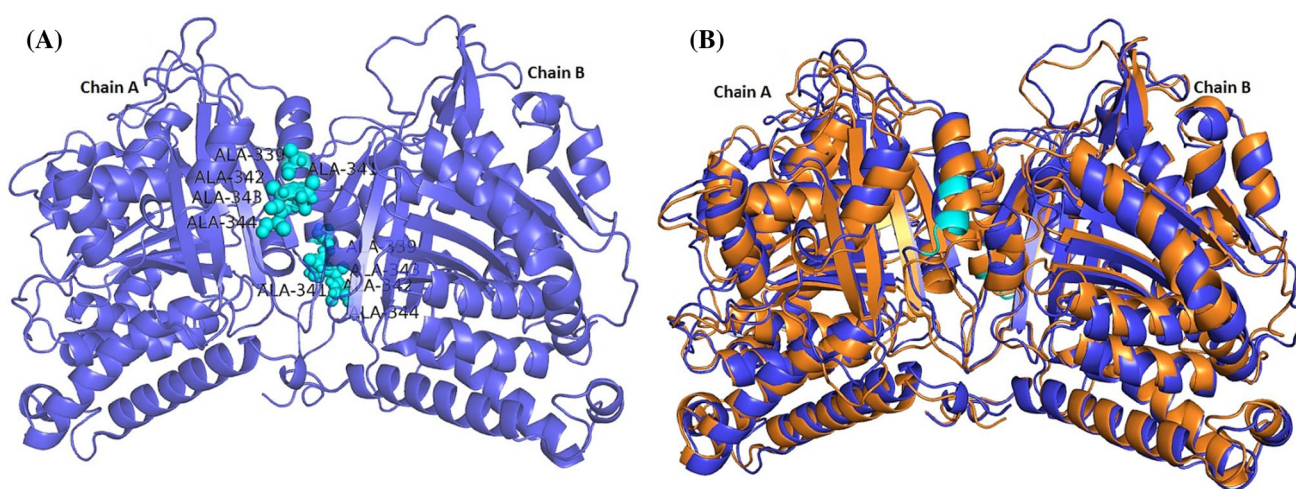
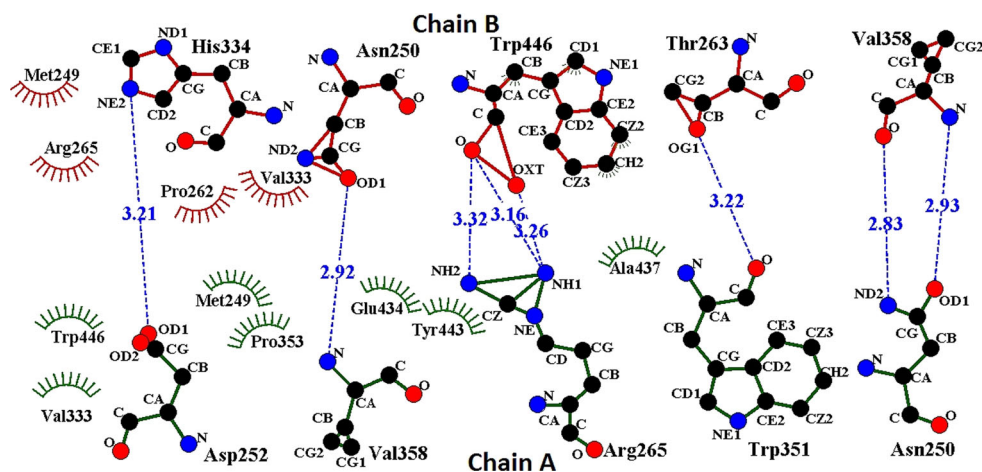


**Fig. 8** Mutant structure of  $\gamma$ - $\gamma$  dimer. Panel 'A' shows the mutant structure of  $\gamma$ - $\gamma$  dimer along with the residues mutated to alanine in cyan colour spheres. Panel 'B' shows the mutated structure of  $\gamma$ -tubulin dimer obtained after 10 ns MD simulation in Amber (blue)

superimposed over the structure of wild type  $\gamma$ -tubulin dimer (Orange) obtained after 10 ns MD simulations in amber. Calculated RMSD was 1.75 Å

**Fig. 9** 2D representation of molecular interactions between the amino acids of the two mutated units of  $\gamma$ - $\gamma$  tubulin (chain 'A' and chain 'B'). Hydrogen bonding residues are shown in green and red for chain A and chain B, respectively. The Dashed lines denote hydrogen bonds, and numbers indicate hydrogen bond lengths in Å. Hydrophobic interactions are shown as arcs with radial spokes. The Figs was made using Dimplot [52]



mutating a stretch of five polar amino acids (Arg339, Arg341, Glu342, Arg343 and Lys344) to alanine. The results from MM-PBSA and MM-GBSA showed a significant drop in the binding affinity between  $\gamma$ - $\gamma$  tubulin interactions. To test whether a subset of these mutant proteins can support life, experimental alanine scanning mutagenesis was performed and the cDNA encoding the mutant and the endogenous fission yeast  $\gamma$ -tubulin (*gtb1*) gene was replaced with the mutant  $\gamma$ -tubulin gene (*TUBG1*) in haploid cells. We found that the  $\gamma$ - $\gamma$  tubulin mutant (*gtb1*-alanine-*TUBG1*) that was predicted to disrupt interactions was unable to support growth in the absence of endogenous *gtb1*<sup>+</sup> (referred to as recessive lethal). These findings thus correlate well with our computer predictions of important residues for  $\gamma$ -tubulin interactions.

**Acknowledgments** The work was supported partially by funding from the United States of America National Institutes of Health R01-CA095317 (H.C. Joshi) and NRSA-GM18037 (T.W. Hendrickson). The authors are thankful to Prof. B. Jayaram and the staff of the SCFBio lab at IIT-Delhi for providing the access to their supercomputing facility to perform MD simulation. Authors are also thankful to Jaypee University of Information Technology for providing fellowship to Miss. Charu Suri.

## References

- Oakley BR, Oakley CE, Yoon Y, Jung MK (1990)  $\gamma$ -Tubulin is a component of the spindle pole body that is essential for microtubule function in *Aspergillus nidulans*. *Cell* 61(7):1289–1301
- Zheng Y, Jung MK, Oakley BR (1991)  $\gamma$ -Tubulin is present in *Drosophila melanogaster* and *Homo sapiens* and is associated with the centrosome. *Cell* 65(5):817–823
- Stearns T, Evans L, Kirschner M (1991)  $\gamma$ -Tubulin is a highly conserved component of the centrosome. *Cell* 65(5):825–836
- Horio T, Uzawa S, Jung MK, Oakley BR, Tanaka K, Yanagida M (1991) The fission yeast gamma-tubulin is essential for mitosis and is localized at microtubule organizing centers. *J Cell Sci* 99(4):693–700
- Joshi HC, Palacios MJ, McNamara L, Cleveland DW (1992)  $\gamma$ -Tubulin is a centrosomal protein required for cell cycle-dependent microtubule nucleation. *Nature* 365:80–83
- Joshi HC (1993)  $\gamma$ -Tubulin: the hub of cellular microtubule assemblies. *BioEssays* 15(10):637–643
- Oakley CE, Oakley BR (1989) Identification of  $\gamma$ -tubulin, a new member of the tubulin superfamily encoded by *mipA* gene of *Aspergillus nidulans*. *Nature* 338:662–664
- Sui H, Downing KH (2010) Structural basis of interprotofilament interaction and lateral deformation of microtubules. *Structure* 18(8):1022–1031
- Rice LM, Montabana EA, Agard DA (2008) The lattice as allosteric effector: structural studies of  $\alpha\beta$ - and  $\gamma$ -tubulin clarify the role of GTP in microtubule assembly. *Proc Natl Acad Sci* 105(14):5378–5383
- Wilson EB (1928) *The cell in development and heredity*, 3rd edn. The Macmillan Co., New York
- Li Q, Joshi HC (1995) Gamma-tubulin is a minus end-specific microtubule binding protein. *J Cell Biol* 131(1):207–214
- Oegema K, Wiese C, Martin OC, Milligan RA, Iwamatsu A, Mitchison TJ, Zheng Y (1999) Characterization of two related *Drosophila*  $\gamma$ -tubulin complexes that differ in their ability to nucleate microtubules. *J Cell Biol* 144(4):721–733
- Zheng Y, Wong ML, Alberts B, Mitchison T (1995) Nucleation of microtubule assembly by a gamma-tubulin-containing ring complex. *Nature* 378(6557):578–583
- Gohlke H, Case DA (2004) Converging free energy estimates: MM-PB (GB) SA studies on the protein–protein complex Ras-Raf. *J Comput Chem* 25(2):238–250
- Gohlke H, Kiel C, Case DA (2003) Insights into protein–protein binding by binding free energy calculation and free energy decomposition for the Ras-Raf and Ras-RalGDS complexes. *J Mol Biol* 330(4):891–913
- Zoete V, Meuwly M, Karplus M (2005) Study of the insulin dimerization: binding free energy calculations and per-residue free energy decomposition. *Proteins Struct Funct Bioinf* 61(1):79–93
- Michalik L, Zoete V, Krey G, Grosdidier A, Gelman L, Chodanowski P, Feige JN, Desvergne B, Wahli W, Michielin O (2007) Combined simulation and mutagenesis analyses reveal the involvement of key residues for peroxisome proliferator-activated receptor $\alpha$  helix 12 dynamic behavior. *J Biol Chem* 282(13):9666–9677
- Stites WE (1997) Protein-protein interactions: interface structure, binding thermodynamics, and mutational analysis. *Chem Rev* 97(5):1233–1250
- Zoete V, Michielin O (2007) Comparison between computational alanine scanning and per-residue binding free energy decomposition for protein–protein association using MM-GBSA: application to the TCR-p-MHC complex. *Proteins Struct Funct Bioinf* 67(4):1026–1047

20. Kollman PA, Massova I, Reyes C, Kuhn B, Huo S, Chong L, Lee M, Lee T, Duan Y, Wang W (2000) Calculating structures and free energies of complex molecules: combining molecular mechanics and continuum models. *Acc Chem Res* 33(12):889–897
21. Onufriev A, Bashford D, Case DA (2000) Modification of the generalized Born model suitable for macromolecules. *J Phys Chem B* 104(15):3712–3720
22. Srinivasan J, Cheatham TE, Cieplak P, Kollman PA, Case DA (1998) Continuum solvent studies of the stability of DNA, RNA, and phosphoramidate-DNA helices. *J Am Chem Soc* 120(37):9401–9409
23. Tsui V, Case DA (2000) Theory and applications of the generalized Born solvation model in macromolecular simulations. *Biopolymers* 56(4):275–291
24. Lafont V, Schaefer M, Stote RH, Altschuh D, Dejaegere A (2007) Protein–protein recognition and interaction hot spots in an antigen–antibody complex: free energy decomposition identifies “efficient amino acids”. *Proteins Struct Funct Bioinf* 67(2):418–434
25. Hess B, Kutzner C, Van Der Spoel D, Lindahl E (2008) GRO-MACS 4: algorithms for highly efficient, load-balanced, and scalable molecular simulation. *J Chem Theory Comput* 4(3):435–447
26. Berendsen H, Postma J, Van Gunsteren W, Hermans J (1981) *Intermolecular Forces*, ed. B Pullman, Reidel, Dordrecht 331
27. Darden T, York D, Pedersen L (1993) Particle mesh Ewald: an  $N \log(N)$  method for Ewald sums in large systems. *J Chem Phys* 98(12):10089–10092
28. Essmann U, Perera L, Berkowitz ML, Darden T, Lee H, Pedersen LG (1995) A smooth particle mesh Ewald method. *J Chem Phys* 103(19):8577–8593
29. Ryckaert J-P, Ciccotti G, Berendsen HJ (1977) Numerical integration of the cartesian equations of motion of a system with constraints: molecular dynamics of  $\langle i \rangle_n \langle i \rangle$ -alkanes. *J Comput Phys* 23(3):327–341
30. Laskowski RA, MacArthur MW, Moss DS, Thornton JM (1993) PROCHECK: a program to check the stereochemical quality of protein structures. *J Appl Crystallogr* 26(2):283–291
31. Ramachandran G, Ct Ramakrishnan, Sasisekharan V (1963) Stereochemistry of polypeptide chain configurations. *J Mol Biol* 7(1):95–99
32. Colovos C, Yeates TO (1993) Verification of protein structures: patterns of nonbonded atomic interactions. *Protein Sci* 2(9):1511–1519
33. Eisenberg D, Lüthy R, Bowie JU (1997) VERIFY3D: assessment of protein models with three-dimensional profiles. *Methods Enzymol* 277:396
34. Case DA, Cheatham TE, Darden T, Gohlke H, Luo R, Merz KM, Onufriev A, Simmerling C, Wang B, Woods RJ (2005) The Amber biomolecular simulation programs. *J Comput Chem* 26(16):1668–1688
35. Pearlman DA, Case DA, Caldwell JW, Ross WS, Cheatham TE III, DeBolt S, Ferguson D, Seibel G, Kollman P (1995) AMBER, a package of computer programs for applying molecular mechanics, normal mode analysis, molecular dynamics and free energy calculations to simulate the structural and energetic properties of molecules. *Comput Phys Commun* 91(1):1–41
36. Cornell WD, Cieplak P, Bayly CI, Gould IR, Merz KM, Ferguson DM, Spellmeyer DC, Fox T, Caldwell JW, Kollman PA (1995) A second generation force field for the simulation of proteins, nucleic acids, and organic molecules. *J Am Chem Soc* 117(19):5179–5197
37. Hornak V, Abel R, Okur A, Strockbine B, Roitberg A, Simmerling C (2006) Comparison of multiple Amber force fields and development of improved protein backbone parameters. *Proteins Struct Funct Bioinf* 65(3):712–725
38. Jorgensen WL, Chandrasekhar J, Madura JD, Impey RW, Klein ML (1983) Comparison of simple potential functions for simulating liquid water. *J Chem Phys* 79(2):926–935
39. Berendsen HJ, Postma JPM, van Gunsteren WF, DiNola A, Haak J (1984) Molecular dynamics with coupling to an external bath. *J Chem Phys* 81(8):3684–3690
40. Honig B, Nicholls A (1995) Classical electrostatics in biology and chemistry. *Science, New Series* 268:1144–1149
41. Massova I, Kollman PA (2000) Combined molecular mechanical and continuum solvent approach (MM-PBSA/GBSA) to predict ligand binding. *Perspect Drug Discovery Des* 18(1):113–135
42. Sitkoff D, Sharp KA, Honig B (1994) Accurate calculation of hydration free energies using macroscopic solvent models. *J Phys Chem* 98(7):1978–1988
43. Guo J, Wang X, Sun H, Liu H, Yao X (2012) The molecular basis of IGF-II/IGF2R recognition: a combined molecular dynamics simulation, free-energy calculation and computational alanine scanning study. *J Mol Model* 18(4):1421–1430
44. Zoete V, Irving M, Michielin O (2010) MM–GBSA binding free energy decomposition and T cell receptor engineering. *J Mol Recognit* 23(2):142–152
45. Hendrickson TW, Yao J, Bhadury S, Corbett AH, Joshi HC (2001) Conditional mutations in  $\gamma$ -tubulin reveal its involvement in chromosome segregation and cytokinesis. *Mol Biol Cell* 12(8):2469–2481
46. Maundrell K (1990) nmt1 of fission yeast. A highly transcribed gene completely repressed by thiamine. *J Biol Chem* 265(19):10857–10864
47. Maundrell K (1993) Thiamine-repressible expression vectors pREP and pRIP for fission yeast. *Gene* 123(1):127–130
48. Paluh J, Clayton D (1996) A functional dominant mutation in *Schizosaccharomyces pombe* RNase MRP RNA affects nuclear RNA processing and requires the mitochondrial-associated nuclear mutation ptp1-1 for viability. *EMBO J* 15(17):4723
49. Horio T, Oakley BR (1994) Human gamma-tubulin functions in fission yeast. *J Cell Biol* 126(6):1465–1473
50. Tsai CJ, Nussinov R (1997) Hydrophobic folding units at protein–protein interfaces: implications to protein folding and to protein–protein association. *Protein Sci* 6(7):1426–1437
51. Davis SJ, Davies EA, Tucknott MG, Jones EY, Van Der Merwe PA (1998) The role of charged residues mediating low affinity protein–protein recognition at the cell surface by CD2. *Proc Natl Acad Sci* 95(10):5490–5494
52. Wallace AC, Laskowski RA, Thornton JM (1995) LIGPLOT: a program to generate schematic diagrams of protein–ligand interactions. *Protein Eng* 8(2):127–134